Septin-dependent compartmentalization of the endoplasmic reticulum during yeast polarized growth

Cosima Luedeke,[1] Stéphanie Buvelot Frei,[1] Ivo Sbalzarini,[2] Heinz Schwarz,[3] Anne Spang,[4] and Yves Barral[1]

[1]Biology Department, Institute of Biochemistry, Swiss Federal Institute of Technology (ETH), ETH-Hönggerberg, 8093 Zürich, Switzerland
[2]Institute of Computational Science, ETH, ETH-Zentrum, 8092 Zürich, Switzerland
[3]Max Planck Institute of Developmental Biology and [4]Friedrich Miescher Laboratory of the Max Planck Society, D-72076 Tübingen, Germany

Polarized cells frequently use diffusion barriers to separate plasma membrane domains. It is unknown whether diffusion barriers also compartmentalize intracellular organelles. We used photobleaching techniques to characterize protein diffusion in the yeast endoplasmic reticulum (ER). Although a soluble protein diffused rapidly throughout the ER lumen, diffusion of ER membrane proteins was restricted at the bud neck. Ultrastructural studies and fluorescence microscopy revealed the presence of a ring of smooth ER at the bud neck. This ER domain and the restriction of diffusion for ER membrane proteins through the bud neck depended on septin function. The membrane-associated protein Bud6 localized to the bud neck in a septin-dependent manner and was required to restrict the diffusion of ER membrane proteins. Our results indicate that Bud6 acts downstream of septins to assemble a fence in the ER membrane at the bud neck. Thus, in polarized yeast cells, diffusion barriers compartmentalize the ER and the plasma membrane along parallel lines.

Introduction

The ER, the major intracellular membrane system of eukaryotes, ensures the biosynthesis of all lipid precursors, as well as the membrane insertion and the translocation through the lipid bilayer of most membrane and secreted proteins (for reviews see Matlack et al., 1998; Meldolesi and Pozzan, 1998; McMaster, 2001; Ma and Hendershot, 2001). As a calcium-storing organelle, the ER plays crucial roles in signal transduction and the regulation of calcium-dependent processes, such as the control of myosin II activity during muscle contraction (Meldolesi and Pozzan, 1998). However, ER function reaches beyond the metabolism and impacts the structural organization of the cell, at least through the formation of the nuclear envelope (Baumann and Walz, 2001). As such, it is "the" eukaryotic organelle par excellence.

The ER is formed of an oxidizing environment enveloped by a single lipid bilayer. It assembles into sheets and reticulated tubules that appear continuous with each other by electron microscopy (Baumann and Walz, 2001). Furthermore, photobleaching experiments showed that ER components freely diffuse throughout the entire ER of fibroblasts (Dayel et al., 1999; Nikonov et al., 2002). Thus, the consensus has emerged that eukaryotic cells contain a single ER. In turn, ultrastructural studies established that the continuous ER membrane is highly organized and forms differentiated domains, such as the nuclear envelope and the rough and smooth ER (Baumann and Walz, 2001). However, we still know little about how these structures differentiate from each other. We also know little about the involvement of the ER in complex cellular processes such as cell polarization and cell division. Particularly, we do not know how the ER is cleaved at or before cytokinesis.

In most cells, the ER is tightly associated with the cytoskeleton, and it colocalizes extensively with microtubules in animal cells (Barr, 2002; Du et al., 2004). This tight association of ER and cytoskeleton suggests that cell polarization might strongly impact on ER organization. Over the last decades, cell polarization has been mainly apprehended as the asymmetric distribution of plasma membrane markers. In epithelial cells, neurons, and yeast, this asymmetry takes the form of functionally and structurally distinct plasma membrane domains that are separated by diffusion barriers (Faty et al., 2002; Boiko and Winckler, 2003). Whether and how the compartmentalization of the plasma membrane affects the internal organization of the cell has not been studied much, and little is known about how cell polarity impinges on ER organization.

The budding yeast *Saccharomyces cerevisiae* has provided an excellent model to study cell polarity and its molecular mechanism (Pruyne and Bretscher, 2000a,b). This unicellular

C. Luedeke and S. Buvelot Frei contributed equally to this paper.

Correspondence to Yves Barral: yves.barral@bc.biol.ethz.ch

Abbreviations used in this paper: FLIP, fluorescence loss in photobleaching; SDK, septin-dependent kinase; WT, wild type.

The online version of this article includes supplemental material.

The Journal of Cell Biology, Vol. 169, No. 6, June 20, 2005 897–908
http://www.jcb.org/cgi/doi/10.1083/jcb.200412143

organism divides by budding; i.e., it polarizes its growth to produce a daughter cell de novo. The restriction of cell growth to the developing bud depends on the polarization of exocytosis and the actin cytoskeleton. Actin cables are nucleated at the bud cortex in a formin-dependent manner and align along the mother-bud axis. These cables serve as tracks for the myosin-dependent delivery of exocytic vesicle to the bud. Thereby, they ensure the polarized delivery of new membrane, cell wall remodeling enzymes, and cell wall material during bud growth. During this process, the yeast plasma membrane is compartmentalized into a bud and a mother domain that are separated by a septin-dependent diffusion barrier (Barral et al., 2000; Takizawa et al., 2000). Septins are GTPases that assemble into membrane-associated filaments. In yeast, these filaments form a ring at the cortex of the bud neck (for review see Faty et al., 2002). Among other functions, this ring establishes the lateral diffusion barrier that helps maintain the compartmentalization of the yeast plasma membrane.

Recent studies suggest that cell polarity not only affects the plasma membrane but also deeper functions of the cell such as protein synthesis. In yeast, at least 24 mRNAs are specifically translated in the bud (Shepard et al., 2003). Localization of these transcripts depends on actin and the type V myosin Myo4 and its binding partner She3 (Jansen, 2001). Little is known about how these mRNAs are maintained in the bud upon transport. However, the fact that at least 18 of them encode membrane proteins (Shepard et al., 2003) suggests that the ER in the bud might play some role in RNA anchoring. In this study, we focused our attention on the impact of cell polarity on the organization of the yeast ER.

Results

The bud and mother ERs form separate diffusion domains

The yeast ER is organized into a reticulate network that covers the cell cortex and is connected with the nuclear envelope by cytoplasmic tubules (Preuss et al., 1991; Prinz et al., 2000). To gain further insights into yeast ER organization, we performed fluorescence loss in photobleaching (FLIP) experiments on cells expressing Sec61-GFP. Sec61 is the major subunit of the translocon and resides in the ER membrane (Gorlich et al., 1992). Upon repeated photobleaching of a small cortical area, fluorescence loss in other ER regions indicates exchange of Sec61-GFP molecules with the bleached area. This technique permits the evaluation of exchange rates between different regions of the ER. A small area of the mother cortex was photobleached in medium- to large-budded cells. As seen in Fig. 1 A (Video 1, available at http://www.jcb.org/cgi/content/full/jcb.200412143/DC1), photobleaching led to rapid fluorescence loss over the entire cortex of the mother cell ($t_{1/2}$ = 14 ± 2 s; Fig. 1 C). Fluorescence was lost with similar kinetics in the perinuclear ER ($t_{1/2}$ = 19 ± 8 s). In contrast, fluorescence decayed slower in the bud ER ($t_{1/2}$ = 119 ± 36 s, n = 8). This phenomenon was fully reproducible and the delay of fluorescence loss in the bud was highly significant (Fig. 1 E). It also did not depend on the existence of absence of ER tubules between the perinuclear ER and the bud cortex (Fig. 1, compare A and B; and Video 2, available

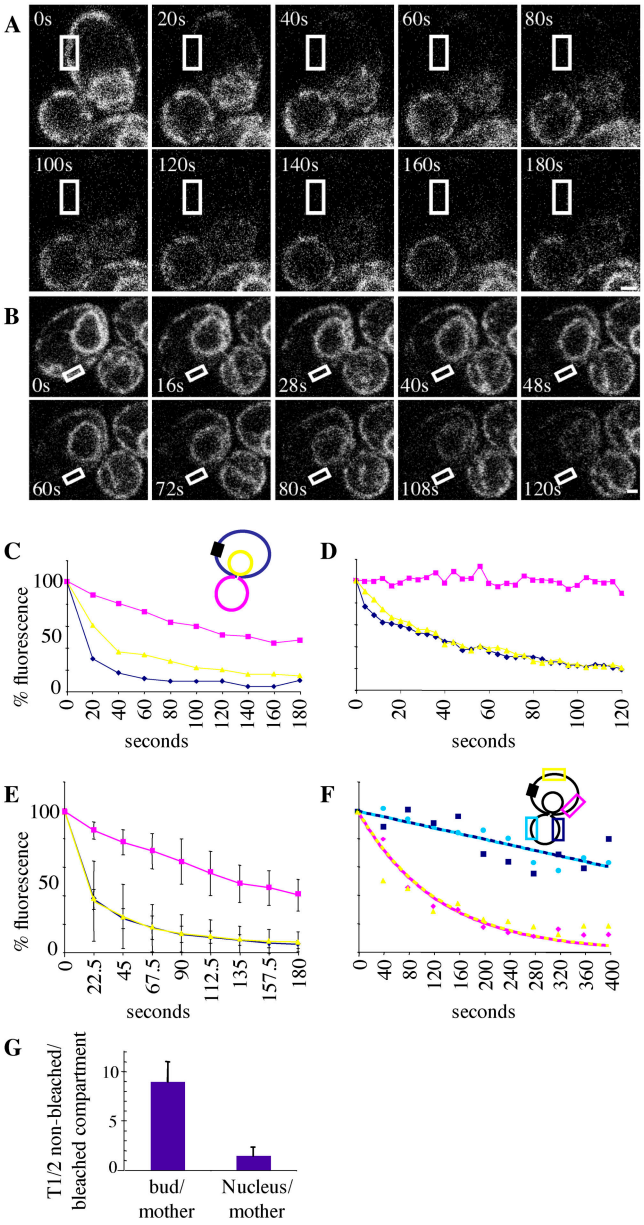

Figure 1. **Dynamics of the translocon subunit Sec61 throughout the yeast ER during metaphase.** (A and B) Diffusion from the mother cortex to the bud cortex is slow. FLIP was performed on a metaphase cell expressing Sec61-GFP. The bleaching region is depicted by an empty rectangle. (A) Pictures were taken every 20 s. (B) Cell showing a cytoplasmic tubule connecting the nucleus and the bud cortex (Video 2). Pictures were taken every 4 s, with relevant frames shown. Note that the movie covers a shorter period of time than in A. (C) Graph showing the kinetics of fluorescence loss for the cell in A. The cartoon depicts the bleaching region (box) and the three areas in which fluorescence was measured (blue, mother cortex; yellow, perinuclear ER; pink, bud ER). (D) Graph for the cell in B. Color code as in C. (E) Graph showing the kinetics of fluorescence loss after averaging eight different FLIP experiments as in A and B. Color code as in C. (F) Diffusion is fast within each compartment. Loss in fluorescence in the cell in Fig. 2 A was measured in four different regions, two on the mother cortex (pink and yellow boxes on the cartoon) and two on the bud cortex (light and dark blue). The yellow and the light blue region are equidistant from the bleaching region. (G) Graph representing the $t_{1/2}$ of the nonbleached compartment over the $t_{1/2}$ of the bleached compartment. Measures were made on the same eight cells as in B. Error bars indicate the SD. Bars, 1 μm. In this and subsequent figures, elapsed times since the beginning of bleaching are indicated in each frame of the movies, in seconds.

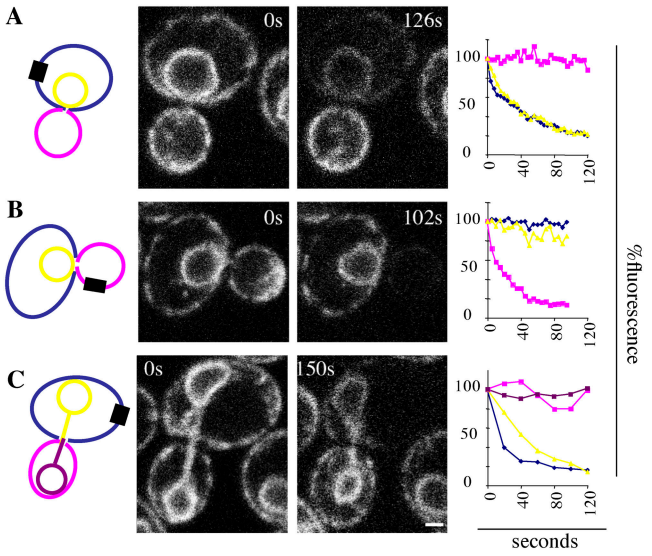

Figure 2. **Dynamics of the translocon subunit Sec61 during a different cell cycle stage.** (A–C) FLIP is applied on cells expressing Sec61-GFP. Color codes and cartoons are as in Fig. 1 C. Relevant frames are shown for each movie. The graphs show the kinetics of fluorescence loss in the three compartments. (A) Photobleaching is applied at the mother cell cortex during metaphase (Video 1). (B) Photobleaching is applied at the bud cortex during metaphase ($n = 4$; Video 3). (C) Photobleaching is applied at the mother cortex during anaphase ($n = 6$; Video 4). Bar, 1 μm.

at http://www.jcb.org/cgi/content/full/jcb.200412143/DC1). The ratio of $t_{1/2}$ of the nonbleached compartment over the $t_{1/2}$ of the bleached compartment is close to 1 for the perinuclear ER (1.4 ± 0.8), but nine times higher (9 ± 1.7; Fig. 1 G) for the bud cortex. Although the $t_{1/2}$ values observed in the different experiments highly depended on the photobleaching protocols used, this ratio remained fairly independent of the size of the bleached area and the duration and intensity of bleaching pulses. Therefore, it is used in the rest of the text to compare experiments and strains. Altogether, these results indicate that Sec61 diffusion is rapid within the mother cortical ER and between the mother cortex and the perinuclear ER. In contrast, Sec61 molecules exchange slowly between mother and bud ERs.

To determine whether the slow loss of fluorescence in the bud is due to its distance to the bleached area, we compared the rate of fluorescence loss between ER regions of the mother and bud that lied at different distances from the bleached area. Fluorescence decayed with similar kinetics in the different domains of the mother cortex (Fig. 1 F, yellow and pink traces). Thus, Sec61-GFP diffusion was instantaneous at the mother cortex, which can be treated as a single compartment. Similarly, the bud cortex also behaved as a single compartment (Fig. 1 F, light and dark blue traces). The region of the bud cortex marked in light blue and the region of the mother cortex marked in yellow (Fig. 1 F) are equidistant from the bleached area. Thus, the fact that these two regions lose fluorescence with distinct kinetics indicated that the difference observed between mother and bud cortices was not due to their different distance to the bleached area.

Translation dramatically slows down the diffusion of Sec61 (Nikonov et al., 2002). Thus, differences in translational activity between mother and bud might cause Sec61 to diffuse slower in the bud than in the mother. This could explain the slow kinetics of fluorescence loss in the bud versus the mother cell. However, photobleaching at the bud cortex (Fig. 2 B and Video 3, available at http://www.jcb.org/cgi/content/full/jcb.200412143/DC1) and FRAP experiments (Fig. S1, available at http://www.jcb.org/cgi/content/full/jcb.200412143/DC1) indicated that Sec61 moved at similar rates in the bud and the mother cell. In these experiments, fluorescence loss was rapid in the bud but slow in the mother. Thus, our FLIP and FRAP data suggest that diffusion of Sec61 through the bud neck is restricted and hence that mother and bud ERs form separate diffusion domains.

A remarkably similar situation was observed for the nuclear envelope during late anaphase. In these cells, exchange between mother and bud cortical ERs remained limited. In addition, the mother cortex exchanged material only with the nuclear half located in the mother cell (Fig. 2 C and Video 4, available at http://www.jcb.org/cgi/content/full/jcb.200412143/DC1; ratio $t_{1/2}$ perinuclear ER mother/$t_{1/2}$ mother = 2.6, $t_{1/2}$ perinuclear ER bud/$t_{1/2}$ mother = 11.6, $t_{1/2}$ bud cortex/$t_{1/2}$ mother = 13.4, $n = 6$). Concomitantly, the perinuclear ER located in the bud also exchanged rapidly but exclusively with the bud cortical ER (unpublished data). This indicates that in late anaphase the yet undivided nucleus behaved as two distinct domains of diffusion, each exchanging Sec61 molecules only with the cortical ER of the cellular domain in which it was located. Thus, diffusion through the bud neck was limited at all times. At least in the case of the nuclear envelope, a lateral diffusion barrier must have restricted the movement of Sec61-GFP within the continuous ER membrane at the bud neck.

Next, we extended our investigations to other ER proteins. The ER membrane proteins GFP-Sec22 and Hmg1-GFP (Fig. 3, A and B) provided results very similar to those obtained with Sec61-GFP. Sec22 is a v-SNARE required for vesicular transport between the ER and the Golgi (Kaiser and Schekman, 1990; Newman et al., 1990) and GFP-Sec22 localizes almost exclusively to the ER. Hmg1 is one of the two yeast isoforms of the 3-hydroxy-3-methylglutaryl-coenzyme A reductase (Qureshi et al., 1976). Thus, the ER is separated into bud and mother domains by an activity that limits the exchange of ER membrane proteins through the bud neck.

The ER lumen is continuous throughout the cell

Different results were obtained with the luminal protein GFP-HDEL. Exchange was rapid between the mother and the bud ER (Fig. 3 C and Video 5, available at http://www.jcb.org/cgi/content/full/jcb.200412143/DC1; upon bleaching in the mother: $t_{1/2}$ in the bud/$t_{1/2}$ in the mother = 2 ± 0.4). GFP-HDEL is targeted to the ER lumen by a signal sequence, while a retrieval sequence (HDEL) ensures ER retention (Pelham, 1991). The fast exchange of GFP-HDEL between mother and bud did not take place through the Golgi because it was not slowed down in the *sec18-1*, *sar1-D32G*, and *cdc48-6* mutants incubated at the restrictive temperature for at least 30 min (Tables I and II and Fig. 3, D and E). Previous studies indicated

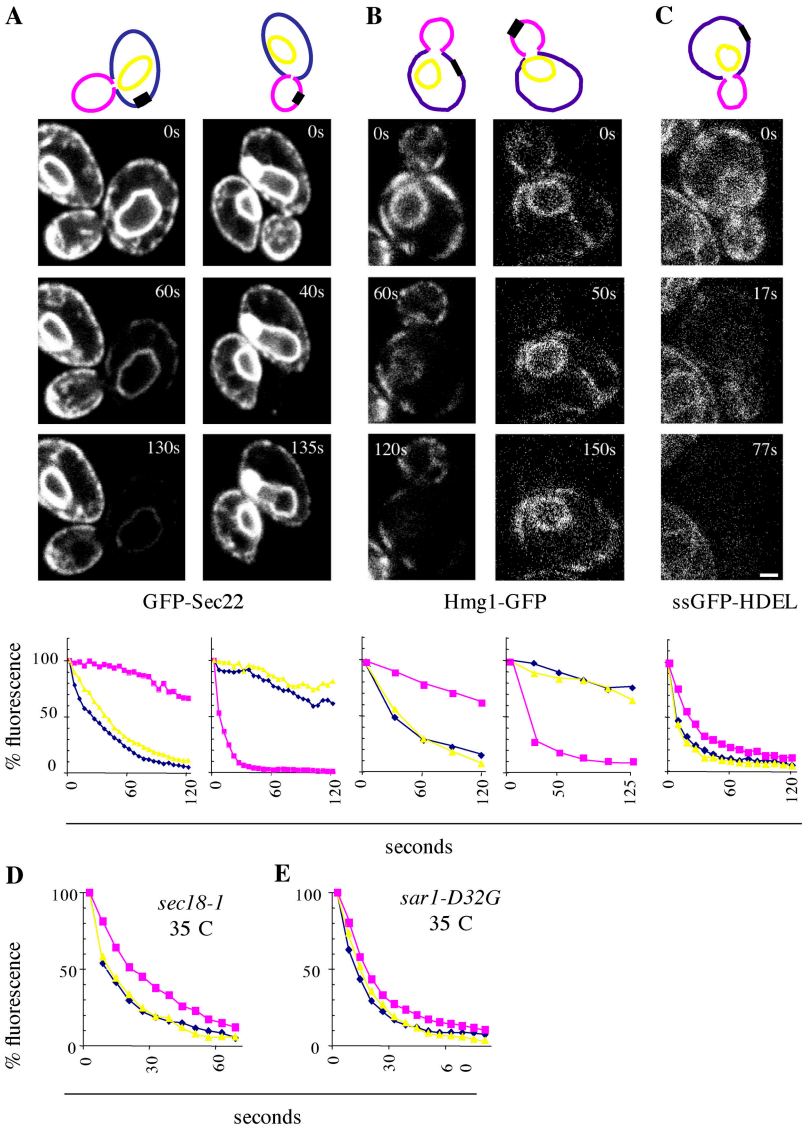

Figure 3. **The diffusion barrier is observed in the membrane of the ER but not in the ER lumen.** (A) FLIP experiments on metaphase cells expressing GFP-Sec22 under the control of the *GAL1* promotor. Photobleaching is applied at the mother (left; $n = 7$) or at the bud cortex (right; $n = 21$). (B) FLIP experiment on cells expressing Hmg1-GFP. Photobleaching is applied at the mother cortex (left; $n = 8$) or bleaching the bud cortex (right; $n = 8$). (C) FLIP experiment on a cell expressing ssGFP-HDEL. Photobleaching is applied at the mother cortex (Video 5), $n = 8$. (A–C) Cartoons and graphs as in Fig. 1 C. Bar, 1 μm. (D) Graph of a FLIP experiment performed on a *sec18-1* mutant cell at restrictive temperature (35°C) bleaching the mother cortex. $n = 8$. (E) Graph of a FLIP experiment performed on a *sar1-D32G* mutant cell at restrictive temperature (35°C) bleaching the mother cortex, $n = 5$.

that these mutations abolish the function of the protein within 10 min at the restrictive temperature. Sec18 is the yeast homologue of NSF and is required for vesicle fusion with target membranes during antero- and retrograde transport between ER and Golgi (Spang and Schekman, 1998). Sar1 is required for vesicle budding at the ER surface (Barlowe et al., 1993). The AAA-ATPase Cdc48 is required for ER homotypic membrane fusion events (Latterich et al., 1995). Thus, none of the known pathways for ER membrane dynamics was involved in GFP-HDEL exchange between the mother and the bud.

Further data supported the view that GFP-HDEL freely diffused throughout the entire ER. First, in wild type (WT) and mutants, the bud ER exchanged half of GFP-HDEL–associated fluorescence with the mother ER in 12 s (Fig. 3 C). These fast kinetics exclude that it depended on vesicular transport. Furthermore, movement of GFP-HDEL and Sec61-GFP throughout the ER required neither ATP nor GTP (Fig. 4 A). Indeed, when the FLIP experiments were performed in cells treated with sodium azide to deplete metabolic energy, no change in the dynamics of GFP-HDEL and Sec61-GFP was observed. This treatment influenced neither exchange of the markers between mother and bud nor the diffusion of either molecule throughout the mother cortex (Fig. 4 A). In contrast, it immediately stopped nuclear movements and the elongation of the nucleus of anaphase cells, indicating that energy depletion was rapid. Therefore, ER membrane fission, fusion, and vesicular trafficking had little impact on the movement of membrane and

Table I. **Quantification of ER distribution in EM pictures**

	Mother WT	Bud WT	Bud neck WT	Mother shs1Δ	Bud shs1Δ	Bud neck shs1Δ
% rough ER	92 ± 3	72 ± 5	3 ± 6	93 ± 3	64 ± 8	91 ± 12
% smooth ER	8 ± 3	28 ± 5	97 ± 6	7 ± 3	36 ± 8	9 ± 12
% surface covered	48 ± 5	75 ± 11	97 ± 5	62 ± 5	79 ± 17	72 ± 27

EM images of medium-budded cells were analyzed using the software ImageJ 1.29. $n = 8$ for WT and 5 for *shs1Δ*. The presence of a ribbon of ribosome-free region close to the cortex indicates the presence of ER. Aligned ribosomes along the ER lumen (Fig. 4 C) indicate rough ER, whereas ribosomes unaligned and not touching each other indicate the presence of smooth ER.

Table II. **List of mutants tested for compartmentalization of the Sec61-GFP marker or the ssGFP-HDEL**

Strain	Comp. Sec61	Comp. HDEL	Protein encoded by WT gene	Localization
WT	+	−		
cdc12-1	−	NT	Septin	Bud neck
cdc12-6	−	NT	Septin	Bud neck
shs1Δ	−	NT	Septin	Bud neck
hsl1Δ	+	NT	SDK	Bud neck
gin4Δ	+	NT	SDK	Bud neck
swe1Δ	+	NT	Septin checkpoint	Bud neck and nucleus
cdc12-6 swe1Δ	−	NT		
hsl1Δ gin4Δ swe1Δ	+/−	NT		
hsl1Δ gin4Δ	+/−	NT		
elm1Δ	+	NT	Kinase and septin organization	Bud neck
kcc4Δ	+	NT	SDK	Bud neck
clb2Δ	+	NT	G2/M cyclin	Nucleus, spindle pole bodies, spindle, and bud neck
sar1-D32G	NT	−	ER vesicle budding	ER
sec18-1	NT	−	Vesicle fusion	ER, Golgi, and vacuole
cdc48-6	+	−	Homotypic fusion	Cytoplasm and nucleus
rvs161Δ	+	NT	Endocytosis	Bud neck
rvs167Δ	+	NT	Actin distribution	Actin cytoskeleton
bnr1Δ	+	NT	Actin cable nucleation	Bud neck
bni1Δ	+	NT	Actin cable nucleation	Bud tip
spa2Δ	+	NT	Cell polarity and cell fusion	Bud tip and bud neck
sph1Δ	+	NT	Polarized growth	Bud tip and bud neck
bud6Δ	−	NT	Polarized growth, bud site selection, and septation	Bud tip and bud neck
pea2Δ	−	NT	Polarized growth	Bud tip and bud neck
hof1Δ	+	NT	Cytokinesis	Bud neck
myo1Δ	+	NT	Cytokinesis	Bud neck
bni5Δ	+	NT	Septin organization	Bud neck
bud3Δ	+/−	NT	Axial budding	Bud neck
bud4Δ	+	NT	Axial budding	Bud neck
axl2Δ	+	NT	Axial budding	Bud, bud neck, and vacuole
axl1Δ	+/−	NT	Axial budding and cell fusion	Bud neck and cell surface
apl3Δ	+	NT	α-Adaptin	Bud neck and cell surface
yap1801Δ	+	NT	Assembly of clathrin cages	Bud, bud neck, and cell surface
yck2Δ	+	NT	Casein kinase I	Bud tip and bud neck
bud14Δ	+	NT	Bud site selection and vacuole maintenance	Bud site, tip, and neck
bem1Δ	+	NT	Cell polarization and bud formation	Bud site, tip, and neck
bem2Δ	+/−	NT	GAP for Rho1	Bud neck and cytoplasm
bem3Δ	+	NT	GAP for Cdc42	Bud site, tip, and neck
bem4Δ	+	NT	Interacts with rho GTPases	Cytoplasm and nucleus
rom2Δ	+	NT	GEF for Rho1	Bud site, tip, and neck

At least six FLIP experiments were performed for each genotype (three movies on two independent segregants). For the mutation affecting the ER barrier, six additional movies were performed. NT, not tested.

luminal proteins within the ER. Thus, the ER must be physically continuous throughout the cell, including the bud neck.

The ER is continuous through the bud neck

To investigate this possibility, we characterized the morphology of the ER by light and electron microscopy. Using confocal microscopy and GFP-HDEL as a marker, the ER lumen was observed to be continuous through the bud neck (Fig. 4 B) of most cells. The ER membrane appeared also continuous at the bud neck when C_6-BODIPY ceramide was used to visualize the ER bilayer (unpublished data). In contrast, both ER membrane markers Sec61-GFP (see Fig. 6 B) and Hmg1-GFP (not depicted) were seen only very rarely and in those cases only transiently at the bud neck (e.g., Fig. 1 B, Sec61-GFP at 28 s). The difference between the luminal and the ER membrane markers was obvious when GFP-HDEL was coexpressed with Hmg1-CFP, in which case an ER domain labeled with GFP and devoid of CFP was observed at the bud neck (Fig. 4 B). Thus, our data indicate that the ER is continuous through the bud neck but that the ER membrane at this location is different from the rest of the ER membrane because it extensively lacks classical ER membrane proteins such as Sec61 and Hmg1.

Analysis of ER organization by high pressure freezing EM led to similar conclusions (Fig. 4 C). In these images, the ER lumen is apparent as a ribosome-free ribbon around the nucleus and at the cell cortex. ER tubules are also observed in the cytoplasm, some of which emerge from the cortical or the perinuclear ER. In rare instances, these ER tubules linked the

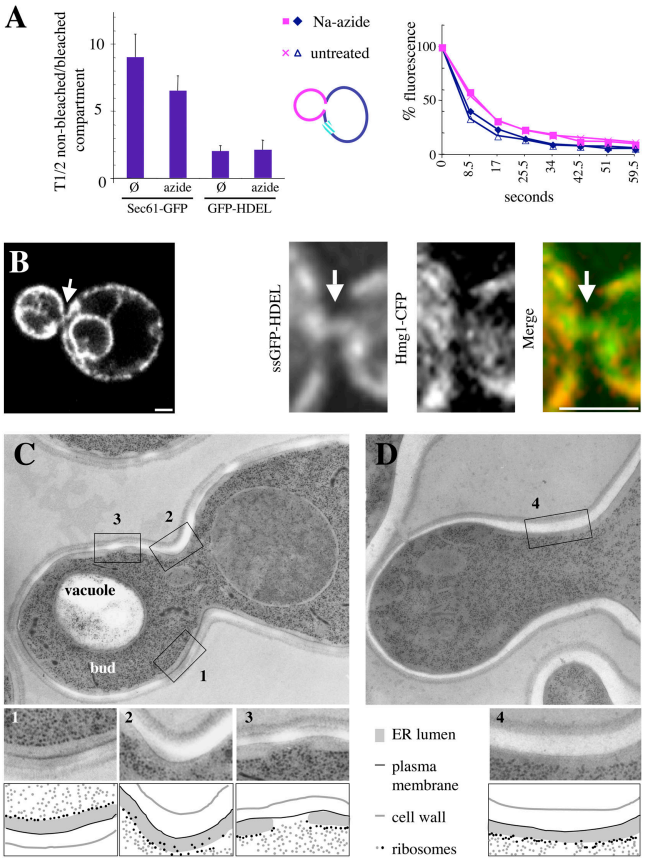

Figure 4. **The ER is continuous through the bud neck and forms a septin-dependent smooth ER structure at the bud neck.** (A) Photobleaching was applied to WT cells expressing Sec61-GFP or ssGFP-HDEL treated or not with 0.1% NaN_3 for 15 min. The left panel shows the ratios of the $t_{1/2}$ of the nonbleached over the $t_{1/2}$ of the bleached compartment for the indicated conditions. The right panel shows a representative kinetics of fluorescence loss over time for cells expressing ssGFP-HDEL treated or not with NaN_3. $n = 8$ for each condition. Error bars indicate the SD. (B) Spinning disk confocal images through the bud neck of a yeast cell expressing ssGFP-HDEL. Blow up of the neck of a cell expressing ssGFP-HDEL (green in the overlay) and Hmg1-CFP (red in the overlay). Arrows point at GFP-HDEL localization to the bud neck. Bars, 1 μm. (C) Transmission electron microscopy images of the bud neck of a WT yeast cell. Magnifications are shown for the indicated regions. (D) Transmission election microscopy images of the bud neck of a *shs1Δ* mutant cell. Magnification is shown for the bud neck. Explanatory schemes are shown below each close up.

perinuclear and cortical ERs. In all images, a ribosome-free ribbon continuous with the mother and bud cortical ERs was observed along the plasma membrane of the bud neck. This ribbon had the same thickness as the ER lumen at other cortical locations and around the nucleus. It was still observed in *shs1Δ* (Fig. 4 D) and *cdc12-6* cells shifted to the restrictive temperature for an hour. Within 2 min of the shift, the *cdc12-6* septin allele causes the complete disassembly of the septin ring at the bud neck (Dobbelaere et al., 2003; Dobbelaere and Barral, 2004), which causes the dispersion of all known bud neck proteins (Gladfelter et al., 2001). Shs1/Sep7 is a nonessential septin in yeast (Carroll et al., 1998; Mino et al., 1998). Because the same ribbon is observed independent of septin presence, this ribbon must correspond to the ER lumen and not to the exclusion of ribosomes by septin-specific structures. Thus, both EM and light microscopy images were consistent with the ER being continuous through the bud neck.

The smooth ER at the bud neck is septin dependent

Analysis of ribosome arrangement along the ER surface showed the existence of both rough and smooth ER. Ribosomes were well aligned along most of the ER at the mother and bud cortex, which is consistent with the presence of mainly rough ER at these locations (Fig. 4 C, inset 1). In contrast, ribosomes failed to align along the bud neck ER, indicating the presence of smooth ER (Fig. 4 C, inset 2). Furthermore, although the ER did not cover the entire inner surface of the plasma membrane in the bud and the mother, it nearly covered the entire bud neck cortex of WT cells (Fig. 4 C). Quantitative analysis of ER organization (Table I) confirmed that the rough ER was predominant at the mother and bud cortices, whereas the bud neck contained almost exclusively smooth ER. These studies also indicated that the bud neck was reproducibly enriched in ER. These data are in agreement with the exclusion of Sec61-GFP but not GFP-HDEL from the bud neck. Thus, light and electron microscopy data indicate that the tubular cortical ER observed at the mother and bud cortices turns into a ring of smooth ER at the bud neck (see Fig. 7).

Comparison of EM images obtained with the WT and the septin mutant suggested that septins play an important role in the organization of the ER membrane at the bud neck. Indeed, in the *cdc12-6* cells shifted to the restrictive temperature, and in the cells lacking Shs1/Sep7, ribosomes nicely aligned along the ER lumen, which was no longer continuous. Thus, differentiation of the ER membrane at the bud neck depended on septin function.

Analysis of the diffusion data by in silico modeling

Analysis of ER structure by light and electron microscopy as well as our FLIP data with GFP-HDEL indicated that the yeast ER, like the ER of mammalian cells, is a single and continuous physical entity. However, our FLIP results also indicated that the diffusion of membrane proteins is slowed down in the bud neck. These data suggest the existence of a lateral diffusion barrier in the ER membrane at the bud neck. Alternatively, geometrical constraints might favor the diffusion of luminal over membrane proteins through the bud neck. Comparison of the exchange rate between mother and bud ER for luminal and membrane proteins is not trivial: diffusion in the volume of the ER lumen is not directly comparable to that in the surface of the ER membrane. To circumvent this problem, we developed an in silico modeling approach (see the online supplemental material and Figs. S2 and S3, available at http://www.jcb.org/cgi/content/full/jcb.200412143/DC1). In this model, the exchange between the mother cortical and the perinuclear ERs was set as a standard for the codiffusion of luminal and membrane markers. This analysis indicated that even after standardization the exchange rate of the membrane protein at the bud neck was still reduced by a factor 16 relative to that of the soluble marker. Two models can account for this reduction: either

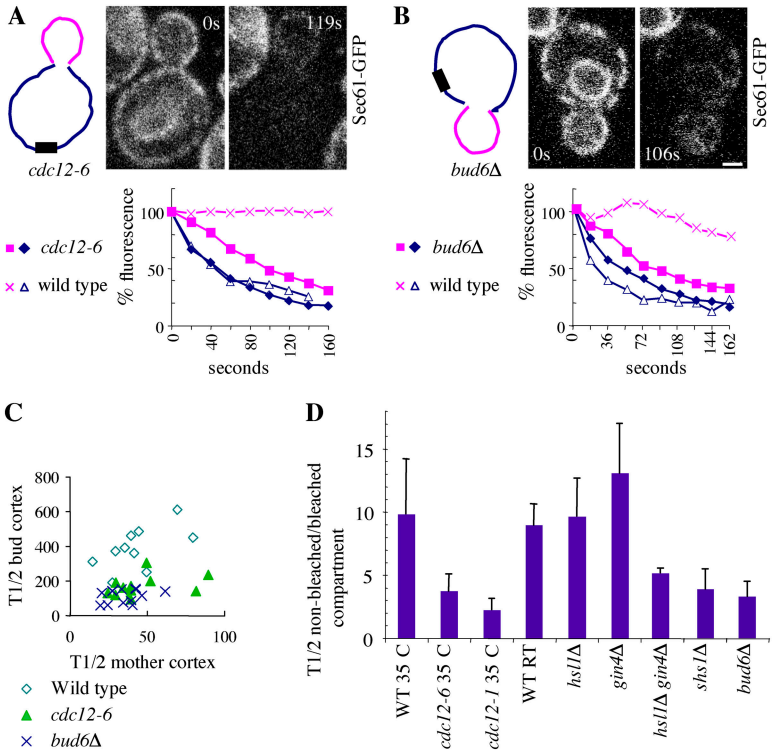

Figure 5. **ER compartmentalization depends on the septins, the SDKs, and Bud6.** (A) FLIP experiment on a *cdc12-6* cell expressing Sec61-GFP. Photobleaching was applied to the mother cortex. Two frames are shown. The graph shows the kinetics of fluorescence loss at the mother cortex in a WT and a *cdc12-6* cell (Video 6) at 35°C (the restrictive temperature for *cdc12-6*); $n = 7$. (B) FLIP experiment on a *bud6Δ* cell expressing Sec61-GFP. Photobleaching was applied at the mother cortex. Relevant frames are shown. The graph shows the kinetics of fluorescence loss in a WT and a *bud6Δ* cell (Video 7) at 22°C. $n = 18$. Bar, 1 μm. (C) Half-times of fluorescence loss in the mother cortex are plotted against those in the bud ER for WT, *cdc12-6*, and *bud6Δ* cells. Each point represents one individual experiment. (D) The ratio of fluorescence decay ($t_{1/2}$) in the nonbleached (bud) versus bleached (mother cortex) compartment is shown for cells of the indicated genotypes. $n \geq 8$. Error bars indicate the SD.

the morphology of the connections offers a larger volume/surface ratio at the bud neck and thereby favors the exchange of the soluble protein over that of the membrane bound, or the diffusion constant is specifically reduced in the membrane. The first model predicts that the connections between mother and bud cortical ERs should be 16 times thicker than those between cortical and perinuclear ER, which is in contradiction to our EM data. Thus, the second model is most likely correct. Our data indicate the existence of a diffusion barrier slowing down the diffusion of proteins in the ER membrane at the bud neck. This conclusion fits with the existence of a differentiated ER membrane at the same location. Thus, we concluded that a diffusion barrier compartmentalized the ER membrane into mother and bud diffusion domains.

Septins, septin-dependent kinases (SDKs), and Bud6 are required for the diffusion barrier

Next, we investigated the molecular basis of this diffusion barrier. Most events at the bud neck depend on septins. Furthermore, our EM data indicated that the smooth ER at the bud neck was disrupted in septin mutants. Thus, we investigated whether the septin ring was involved in the separation of the ER membrane into distinct diffusion domains. *SEC61-GFP cdc12-6* cells shifted to the restrictive temperature (35°C) for at least 15 min were subjected to FLIP studies. In these cells, fluorescence loss in the unbleached compartments (the bud) was only slightly delayed compared with that in the bleached compartment (Fig. 5, A and C; and Video 6, available at http://www.jcb.org/cgi/content/full/jcb.200412143/DC1; $t_{1/2}$ in the bud/$t_{1/2}$ in the mother = 3.7 ± 1.4, $n = 13$, in *cdc12-6* vs. 9.8 ± 4.4 in WT, $n = 7$). Similar results were obtained in cells where septin ring assembly was impaired by the *cdc12-1* mutation and in cells lacking Shs1 (Fig. 5 D). In all the FLIP movies, the frequency of cytoplasmic ER tubules connecting mother and buds was not increased in septin mutants compared with WT (e.g., ER tubule growing through the bud neck appeared in 10.4% of the frames of movies of *shs1Δ* cells, $n = 77$ frames, vs. 13.4% in movies of WT cells, $n = 88$ frames), demonstrating that enhanced exchange through the neck of *shs1Δ* cells was not due to an increased number of cytoplasmic connections. Together, these results indicated that ER compartmentalization depended on septin function. The lack of compartmentalization was not due to the cell cycle delay caused by septin defects because compartmentalization was not restored in *cdc12-6 swe1-Δ* cells. The *swe1-Δ* mutation releases the cell cycle block caused by septin defects (Barral et al., 1999; Shulewitz et al., 1999; Longtine et al., 2000).

During budding, the septin ring recruits to the bud neck many proteins involved in actomyosin ring assembly, chitin deposition, cell cycle progression, and spindle positioning (DeMarini et al., 1997; Bi et al., 1998; Lippincott and Li, 1998; Barral et al., 1999; Shulewitz et al., 1999; Segal et al., 2000; Kusch et al., 2002; Longtine and Bi, 2003). Using our FLIP assay, we tested whether any of 30 bud neck proteins representative of these different functions would play any role in ER compartmentalization (Table II). Partial defects were observed in cells lacking both SDKs, Hsl1 and Gin4, simultaneously (Fig. 5 D and Table II). Again, these defects were not due to over-activation of the Swe1 kinase (Table II). SDKs are involved in signaling downstream of septins. In addition, Gin4 is required for proper septin ring assembly, whereas Hsl1 is not

(Longtine et al., 2000; Dobbelaere et al., 2003). Because cells lacking Gin4 alone are not defective in ER compartmentalization, septin organization defects do not account for the compartmentalization defect observed in the *hsl1Δ gin4Δ* double mutant. These results suggest that SDKs act redundantly and downstream of septins on ER organization. They might modify ER proteins at the bud neck.

In addition to SDKs, only Bud6 and Pea2 were involved in ER compartmentalization. In *bud6Δ* and *pea2Δ* cells the loss of compartmentalization was similar to that caused by septin mutations (Table II; Fig. 5, B–D; and Video 7, available at http://www.jcb.org/cgi/content/full/jcb.200412143/DC1). Bud6 (Amberg et al., 1997), which is a peripheral membrane protein, has been implicated in actin polarization, microtubule interaction with the cell cortex (Segal et al., 2000), and bud site selection in diploid cells. Together with Pea2, it is a component of the polarizome (Sheu et al., 2000), a complex that also contains either of the formins Bni1 and Bnr1, and the polarity factors Spa2 and Sph1. Analysis of ER compartmentalization in *bni1Δ, bnr1Δ, spa2Δ*, and *sph1Δ* cells showed no defect. Thus, the role of Bud6 and Pea2 in ER compartmentalization appeared not to be shared by the other components of the polarizome. Furthermore, like *shs1Δ*, the *bud6*Δ mutation did not increase the number of cytoplasmic ER tubules connecting mother and bud (tubules were present in 11.4% of the frames of *bud6Δ* movies, $n = 138$ frames, vs. 13.4% in WT movies). Thus, the stimulation of exchange between the mother and the bud in *bud6*Δ cells was due to a compartmentalization defect and not to an increased number of ER tubules.

Bud6 acts downstream of the septins

Several lines of evidence suggest that Bud6 acts downstream of septins in ER compartmentalization. First, analysis of septin organization using Cdc12-GFP, Cdc3-GFP, or Shs1-GFP as reporters indicated that the *bud6Δ* mutation did not noticeably affect septin organization (unpublished data). Furthermore, investigation of the localization of Ist2-GFP and Spa2-GFP, which both require a functional septin ring to maintain their asymmetric localization to the cortex of large budded cells (Barral et al., 2000; Takizawa et al., 2000), indicated that the septin-dependent diffusion barrier at the plasma membrane was not affected in *bud6Δ* cells (Fig. 6 A and not depicted). Thus, *bud6Δ* does not generally interfere with septin function. Second, investigation of Bud6 localization in the *shs1Δ* strain indicated that Bud6 failed to accumulate (Fig. 6 C, top) or accumulated to a lesser extent (Fig. 6 C, bottom) at the bud neck of small and medium budded cells, consistent with Huisman et al. (2004). These data suggest that Bud6 acts downstream of septins for the compartmentalization of the ER membrane. Remarkably, Sec61-GFP was still excluded from the bud neck of all *bud6Δ* cells (Fig. 6 B), in contrast to what we observed in the *shs1Δ* and *cdc12-6* cells (Fig. 6 B and compare Videos 8 and 9, available at http://www.jcb.org/cgi/content/full/jcb.200412143/DC1). Altogether, these data suggest that septins have two independent effects on ER organization at the bud neck cortex. They govern on one hand the exclusion of the translocon and the formation of a smooth ER domain, and on the other hand the assembly of a Bud6-dependent barrier that limits the diffusion of ER membrane proteins.

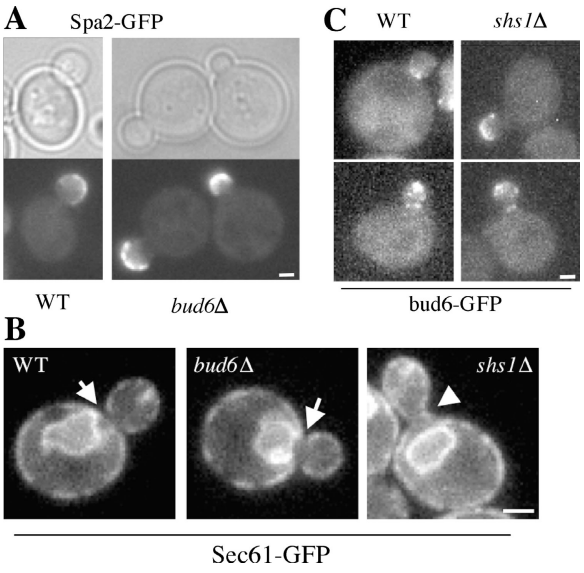

Figure 6. **Bud6 acts downstream of the septins to establish the ER compartmentalization barrier.** (A) The plasma membrane is compartmentalized in *bud6Δ* mutant cells. WT and *bud6Δ* mutant cells expressing Spa2-GFP at the endogenous locus were grown to mid-log on rich medium and then resuspended in nonfluorescent medium. Representative pictures are shown of the localization of Spa2 in small and medium budded cells. (B) *shs1Δ* and *bud6Δ* have different effects on the exclusion of Sec61 from the bud neck. Images of WT, *bud6Δ*, and *shs1Δ* mutant cells expressing Sec61-GFP. Serial sections were taken throughout a budded cell. The section through the bud neck is shown. Arrows point at the discontinuity in Sec61-GFP localization at the bud neck of WT and *bud6Δ* cells. The arrowhead points at Sec61-GFP continuity at the bud neck of the *shs1Δ* cells. The three-dimensional reconstruction of the ER in WT and *shs1Δ* cells are shown in Videos 8 and 9, respectively. (C) Bud6 localization to the bud neck in a small-budded cell is impaired in *shs1Δ* cells. Projection of a z-stack of WT and *shs1Δ* cells expressing bud6-GFP. Bars, 1 μm.

Discussion

In this study, we used photobleaching techniques to investigate ER organization in polarized yeast cells. The diffusion of all tested markers was very fast within the different parts of the ER; i.e, within the ER at the mother cortex, at the bud cortex, and in the nuclear envelope. Remarkably, the yeast ER membrane was separated into distinct domains that reflected cell polarization. This compartmentalization is evidenced by the observation that ER membrane proteins such as the translocon subunit Sec61, the 3-hydroxy-3-methylglutaryl-coenzyme A reductase Hmg1, and the SNARE Sec22 all diffuse very rapidly throughout the bud and mother cortical ERs, but exchange only slowly between these two domains.

Two models can account for such a compartmentalization: either the yeast ER is physically discontinuous, or a diffusion barrier is present within the continuous membrane of the ER at the bud neck. In the first case, residual exchange of ER membrane proteins between the mother and bud must depend on either vesicular transport or transient fusion events. Furthermore, luminal proteins should also be compartmental-

ized. Our data invalidate both predictions. Indeed, diffusion kinetics of the luminal marker GFP-HDEL and morphological analyses at both the light and electron microscopy levels indicate that the ER lumen is continuous throughout the bud neck. Furthermore, exchange of Sec61 and GFP-HDEL between the mother and the bud was due to passive diffusion because it depended neither on the major players of ER membrane trafficking nor on metabolic energy. Thus, the ER is a physically continuous organelle in yeast like in mammalian cells, and its membrane, but not its lumen, is compartmentalized by a diffusion barrier. Our observation that the membrane of the nuclear envelope is also compartmentalized in late anaphase supports this conclusion, as it indicates that ER compartmentalization at the bud neck does not necessarily require the discontinuity of the ER membrane.

The barrier model was supported by the analysis of our quantitative data by in silico modeling. Indeed, this approach demonstrated that compartmentalization of the membrane markers could not be explained by morphological parameters. The barrier model was also supported by our morphological studies. Indeed, we observe that a specialized ER membrane forms at the bud neck, which is both morphologically (it is a sheet instead of tubules) and structurally different from the rest of the cortical ER. Thus, we conclude that a diffusion barrier compartmentalizes the ER membrane along the same lines as those compartmentalizing the plasma membrane of budded yeast cells. To our knowledge, this is the first report of such an intricate relationship between the organization of the ER and that of the plasma membrane.

What could be the cellular function of this complex ER organization? We see two possibilities: (1) the specialized ER domain at the bud neck might have functions related to cell cleavage and/or (2) the separation of the bud and mother cortical ER membranes might provide support for cell polarization.

At the site of division, a specialized ER domain could play two distinct roles. First, this ER domain might serve as a calcium-storing structure involved in the control of actomyosin contraction. This ER domain could work like the sarcoplasmic reticulum of muscle cells in the control of muscle contraction. In support of this idea, septin defects, which cause the loss of the ring of smooth ER, slow down actomyosin ring contraction during cytokinesis (Dobbelaere and Barral, 2004). However, the isolation of mutants that specifically abrogate the formation of the ring of smooth ER at the bud neck will be required to investigate this possibility more rigorously. Second, the ring of smooth ER might be required for ER cleavage at cytokinesis. Further studies will be required to investigate the timing, control, and mechanism of ER cleavage before the completion of cytokinesis.

The compartmentalization of the ER membrane might also play some roles in cell polarity. For example, it could help restrict the synthesis of specialized membrane proteins to one cellular compartment. Most mRNAs that specifically localize to the yeast bud encode membrane proteins and must be translated at the ER surface (Shepard et al., 2003). Thus, ER compartmentalization might help maintain the localized mRNAs in the bud. This mRNA–ER connection seems strengthened by the observation that mRNA and ER transport to the bud neck both involve the type V myosin Myo4 and its associated factor She3 (Estrada et al., 2003). Remarkably, She3 localizes to the bud ER specifically, suggesting that ER compartmentalization might indeed support some structural and functional asymmetry of the ER. However, due to the leakiness of the barrier indicated by our data, it is unclear which kind of asymmetry it helps maintain. Indeed, even though membrane proteins diffused much slower through the bud neck than through the bud or mother cortex, they did eventually translocate from one domain to the other. Thus, the ER diffusion barrier alone cannot maintain very long the asymmetric distribution of polarized factors. Consistently, it has been shown for several products of asymmetrically localized mRNAs that they do not maintain an asymmetric distribution (Shepard et al., 2003), particularly those that are residents of the ER membrane. However, some other products of polarized mRNAs do maintain an asymmetric distribution, the prototype of which is the plasma membrane protein Ist2. In the case of these products, it might be crucial that the ER diffusion barrier slows down their dispersion before they exit the ER, en route to the plasma membrane. Indeed, at least in the case of Ist2, the final localization of the product is determined by the localization of the mRNA (Takizawa et al., 2000). This would not be possible if the product would freely diffuse through the entire ER. Thus, one function of the diffusion barrier in the ER membrane at the bud neck might be to slow down the diffusion to the mother cortex of both polarized mRNAs and their product. Thereby, it permits dynamic processes, such as the movement of Ist2 to the plasma membrane, to remain asymmetric, whereas slower events become isotropic. These observations are reminiscent of the situation recently described in *Drosophila melanogaster* embryos, where the localization of the *Gurken* mRNA determines where at the surface of the embryo this growth factor–like signaling molecule is being secreted (Herpers and Rabouille, 2004). It will be interesting to investigate whether diffusion barriers compartmentalize the ER membrane of the *D. melanogaster* embryo to ensure the accuracy of *Gurken* targeting, and perhaps to also ensure that each of the distinct nuclei acquire and maintain a distinct identity despite being all in the same cytoplasm. Indeed, the division of the ER might support the organization of the entire cytoplasm into distinct domains, such as during the polarization of yeast cells. Thus, we suggest that the ER might play more profound roles in cellular organization than previously anticipated.

The observation that a diffusion barrier compartmentalizes the ER membrane opens two mechanistic questions: (1) what is the molecular nature of this barrier, and (2) how is it localized to the bud neck? Remarkably, we found only few of the known bud neck proteins to be involved in ER compartmentalization. Thus, the identified candidates might act in a very specific manner.

On the septin side, both disruption of the entire ring and elimination of the nonessential septin Shs1/Sep7 dramatically affected both the ER diffusion barrier and the accumulation of smooth ER in the bud neck. Because the *shs1Δ* mutation does not dramatically affect cell viability, septin ring assembly, and morphology (Carroll et al., 1998; Mino et al., 1998), but

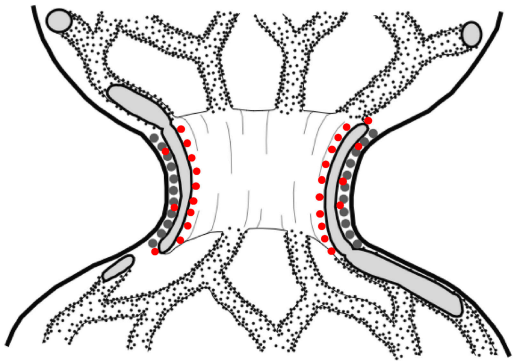

Figure 7. **Model of rough and smooth ER in the bud neck of yeast cells.** Sections through the septin filaments are shown in green. Bud6 localization to the smooth ER is symbolized by red dots.

strongly impacts on ER organization, Shs1 may be specialized for this process. In turn, Bud6 affected only the diffusion barrier and not ER morphology. Thus, the smooth ER at the bud neck does not depend on the presence of the barrier and is not sufficient to form a barrier. Previous data have established that Bud6 is associated with internal membranes (Jin and Amberg, 2000). We propose that Bud6 is a smooth ER protein (Fig. 7), where it might influence protein diffusion.

The role of septins in the recruitment or regulation of ER proteins such as Bud6 might be indirect and mediated at least in part through signaling. Indeed, we found that the SDKs Gin4 and Hsl1 are also involved in the formation of the diffusion barrier. Because SDKs did not seem to function in smooth ER organization, their substrates must be specifically involved in ER compartmentalization. It will be helpful to identify these substrates and to investigate whether Bud6 is one of them. The view that septins act on the ER via signaling mechanisms might explain how they could potentially act at a distance during, for example, the compartmentalization of the nuclear envelope at the bud neck during anaphase.

It is unclear to which extent the observations that we describe here are specific to ER of fungi or relevant for other eukaryotes. At first sight, the fact that the ER of animal cells is mainly cytoplasmic, and not cortical as in fungi, suggests that ER compartmentalization is less likely in metazoans. It will be interesting to perform FLIP experiments on polarized and dividing cells and to investigate whether the role that we ascribe to the cleavage apparatus in the compartmentalization of the yeast ER is conserved during the division of animal cells.

Materials and methods

Strain construction

Yeast strains were constructed by standard genetic techniques. Diploids were isolated on selective medium and subsequently sporulated at 23°C. The background is, unless specified otherwise, S288c. ssGFP-HDEL was expressed from the 2-μm vector pG14 (Lesser and Guthrie, 1993); ssGFP-HDEL has the signal peptide of *CTS1* and the *HDEL* retrieval sequence at its COOH terminus (a gift from E. Bertrand, Centre National de la Recherche Scientifique, Montpellier, France). Strains containing Sec61-GFP (provided by D. Liakopoulos, Swiss Federal Institute of Technology [ETH], Zurich, Switzerland), Spa2-GFP, Bud6-GFP, Hmg1-GFP, or pGAL-GFP-Sec22 were made using the PCR-based integration system (Longtine et al., 1998). The different deletions shown in Table I were obtained from the EUROSCARF deletion collection (S288c) and provided to us by M. Peter (ETH, Zurich, Switzerland). Each time that an effect was observed, the mutation was backcrossed several times into our background. The *hsl1Δ*, *gin4Δ*, *shs1Δ*, and *swe1Δ* strains are isogenic with S288c. Cdc12-GFP was expressed from a centromeric plasmid (Dobbelaere et al., 2003). The *sec18-1* and *cdc48-6* strains were gifts of R. Collins (Cornell University, Ithaca, NY) and S. Jentsch (Max Planck Institute, Münich, Germany), respectively.

FLIP and FRAP experiments

Cells were grown on YPD plates, resuspended in liquid nonfluorescent medium, and immobilized on nonfluorescent medium (Waddle et al., 1996) containing 1.6% agarose. Photobleaching was applied on the area shown on the figures, using a microscope (model LSM510; Carl Zeiss MicroImaging, Inc.) and a Plan-Apochromat 100× objective (NA 1.4). For FRAP, scans were collected at 5-s intervals for a minimum of 120 s using the acquisition software LSM510 (Carl Zeiss MicroImaging, Inc.). Bleaching regions were irradiated with 250 iterations of 50% laser intensity at 30% output of an argon laser (488 nm) and scans were collected with typically 1% laser intensity at the same conditions. All pictures of FLIP experiments shown in the figures were treated to account for the bleaching due to image acquisition, whereas the movies were left untreated.

Pictures shown in Fig. 4 B were taken on a spinning-disc confocal system (Axiovert 200M; Carl Zeiss MicroImaging, Inc.) with a Plan-Apochromat 100× objective. The overlay picture was taken on a DeltaVision microscope (Applied Precision) and deconvolved using the softwox software.

FLIP analysis of septin mutants (*cdc12-1* and *cdc12-6*)

cdc12-1 mutant cells were grown to early log phase at permissive temperature (24°C) in liquid YPD medium and arrested in G1 with 5 μg/ml α-factor for 2.5 h. After removal of α-factor from the medium by washing twice with fresh YPD, cells were mounted on nonfluorescent agarose beds as described in the previous section and immediately shifted to 35°C on a heated stage. FLIP analysis was performed on buds formed after the temperature shift, starting after 30 min. *cdc12-6* cells were grown to mid-log phase on YPD plates at 22°C (permissive), mounted on agarose beds, and shifted to 35°C on the heated stage. FLIP analysis was performed in medium- to large-budded preanaphase cells 30 min after temperature shift.

Quantification of FLIP experiments

Analysis of the FLIP experiments was performed using the ImageJ 1.29 software (http://rsb.info.nih.gov/ij). The loss of fluorescence over time was measured in different regions of interest (usually the mother cortex, bud cortex, and perinuclear ER). In addition, we measured the loss of fluorescence on neighboring control cells to account for the loss due to visualization. Finally, we measured the intensity of the background. The intensity in the region of interest was calculated as (region − background)/(control cell − background) and then put in fractions.

BODIPY staining of ER membranes, light and electron microscopy, and image processing

For BODIPY staining, cells were grown overnight to early to mid-log phase in YPD, harvested, and resuspended in SC media to 5 OD_{600}/ml. The culture was incubated for 10 min at 30°C under agitation. Defatted BSA was added to a final concentration of 5 mg/ml and supplemented with 2.5 μl C6 BODIPY ceramide (4 mM stock in DMSO; Molecular Probes). The cells were incubated for 20 min at 30°C under agitation and mounted for direct inspection. Alternatively, the cells were fixed after the incubation period with 4% formaldehyde. No difference in the staining was detected between life and fixed cells. Light microscopy was performed using either a DeltaVision microscope (DeltaVision Spectris System; Applied Precision) equipped with a Coolsnap HQ camera (Roper Scientific) or an Olympus BX50 equipped with a camera Imago (TiLL Photonics). In all cases, we used 100× objectives of NA 1.4. Deconvolution was performed by a constrained iterative method using the softwox software (Applied Precision). Further image processing was performed using the Photoshop software (Adobe) and was reduced to the optimization of the levels. No gamma adjustments were applied. Unless otherwise indicated, light microscopy was performed at RT (22°C) as described previously (Dobbelaere et al., 2003). EM was performed as described previously (Sandmann et al., 2003).

Model

The quantitative transport model was formulated on the basis of standard physical principles, leading to a system of coupled differential equations. Photobleaching and scanning cycles were modeled as algebraic equations.

Online supplemental material
The quantitative transport model is fully described and assessed in the online supplemental material. Online supplemental material is available at http://www.jcb.org/cgi/content/full/jcb.200412143/DC1.

We are grateful to Markus Aebi and Ari Helenius for helpful discussions. We thank E. Bertrand, R. Collins, S. Jentsch, and M. Peter for strains and constructs; D. Liakopoulos for the Sec61-GFP construct; and J. Dobbelaere for technical help.

This work was supported by the Swiss Federal Institute of Technology (ETH), the Swiss National Science Foundation (Y. Barral), and the Max Planck Society (A. Spang). S. Buvelot Frei was supported by a postdoctoral fellowship from the Roche Foundation and I. Sbalzarini by the ETH Strategic Excellence Project in Computational Science. Y. Barral and A. Spang are European Molecular Biology Organization Young Investigators.

Submitted: 22 December 2004
Accepted: 12 May 2005

References

Amberg, D.C., J.E. Zahner, J.W. Mulholland, J.R. Pringle, and D. Botstein. 1997. Aip3p/Bud6p, a yeast actin-interacting protein that is involved in morphogenesis and the selection of bipolar budding sites. *Mol. Biol. Cell.* 8:729–753.

Barlowe, C., C. d'Enfert, and R. Schekman. 1993. Purification and characterization of SAR1p, a small GTP-binding protein required for transport vesicle formation from the endoplasmic reticulum. *J. Biol. Chem.* 268:873–879.

Barr, F.A. 2002. Inheritance of the endoplasmic reticulum and Golgi apparatus. *Curr. Opin. Cell Biol.* 14:496–499.

Barral, Y., M. Parra, S. Bidlingmaier, and M. Snyder. 1999. Nim1-related kinases coordinate cell cycle progression with the organization of the peripheral cytoskeleton in yeast. *Genes Dev.* 13:176–187.

Barral, Y., V. Mermall, M.S. Mooseker, and M. Snyder. 2000. Compartmentalization of the cell cortex by septins is required for maintenance of cell polarity in yeast. *Mol. Cell.* 5:841–851.

Baumann, O., and B. Walz. 2001. Endoplasmic reticulum of animal cells and its organization into structural and functional domains. *Int. Rev. Cytol.* 205:149–214.

Bi, E., P. Maddox, D.J. Lew, E.D. Salmon, J.N. McMillan, E. Yeh, and J.R. Pringle. 1998. Involvement of an actomyosin contractile ring in *Saccharomyces cerevisiae* cytokinesis. *J. Cell Biol.* 142:1301–1312.

Boiko, T., and B. Winckler. 2003. Picket and other fences in biological membranes. *Dev. Cell.* 5:191–192.

Carroll, C.W., R. Altman, D. Schieltz, J.R. Yates, and D. Kellogg. 1998. The septins are required for the mitosis-specific activation of the Gin4 kinase. *J. Cell Biol.* 143:709–717.

Dayel, M.J., E.F. Hom, and A.S. Verkman. 1999. Diffusion of green fluorescent protein in the aqueous-phase lumen of endoplasmic reticulum. *Biophys. J.* 76:2843–2851.

DeMarini, D.J., A.E. Adams, H. Fares, C. De Virgilio, G. Valle, J.S. Chuang, and J.R. Pringle. 1997. A septin-based hierarchy of proteins required for localized deposition of chitin in the *Saccharomyces cerevisiae* cell wall. *J. Cell Biol.* 139:75–93.

Dobbelaere, J., and Y. Barral. 2004. Spatial coordination of cytokinetic events by compartmentalization of the cell cortex. *Science.* 305:393–396.

Dobbelaere, J., M.S. Gentry, R.L. Hallberg, and Y. Barral. 2003. Phosphorylation-dependent regulation of septin dynamics during the cell cycle. *Dev. Cell.* 4:345–357.

Du, Y., S. Ferro-Novick, and P. Novick. 2004. Dynamics and inheritance of the endoplasmic reticulum. *J. Cell Sci.* 117:2871–2878.

Estrada, P., J. Kim, J. Coleman, L. Walker, B. Dunn, P. Takizawa, P. Novick, and S. Ferro-Novick. 2003. Myo4p and She3p are required for cortical ER inheritance in *Saccharomyces cerevisiae*. *J. Cell Biol.* 163:1255–1266.

Faty, M., M. Fink, and Y. Barral. 2002. Septins: a ring to part mother and daughter. *Curr. Genet.* 41:123–131.

Gladfelter, A.S., J.R. Pringle, and D.J. Lew. 2001. The septin cortex at the yeast mother-bud neck. *Curr. Opin. Microbiol.* 4:681–689.

Gorlich, D., S. Prehn, E. Hartmann, K.U. Kalies, and T.A. Rapoport. 1992. A mammalian homolog of SEC61p and SECYp is associated with ribosomes and nascent polypeptides during translocation. *Cell.* 71:489–503.

Herpers, B., and C. Rabouille. 2004. mRNA localization and ER-based protein sorting mechanisms dictate the use of transitional endoplasmic reticulum-golgi units involved in gurken transport in *Drosophila* oocytes. *Mol. Biol. Cell.* 15:5306–5317.

Huisman, S.M., O.A. Bales, M. Bertrand, M.F. Smeets, S.I. Reed, and M. Segal. 2004. Differential contribution of Bud6p and Kar9p to microtubule capture and spindle orientation in *S. cerevisiae*. *J. Cell Biol.* 167:231–244.

Jansen, R.P. 2001. mRNA localization: message on the move. *Nat. Rev. Mol. Cell Biol.* 2:247–256.

Jin, H., and D.C. Amberg. 2000. The secretory pathway mediates localization of the cell polarity regulator Aip3p/Bud6p. *Mol. Biol. Cell.* 11:647–661.

Kaiser, C.A., and R. Schekman. 1990. Distinct sets of SEC genes govern transport vesicle formation and fusion early in the secretory pathway. *Cell.* 61:723–733.

Kusch, J., A. Meyer, M.P. Snyder, and Y. Barral. 2002. Microtubule capture by the cleavage apparatus is required for proper spindle positioning in yeast. *Genes Dev.* 16:1627–1639.

Latterich, M., K.U. Frohlich, and R. Schekman. 1995. Membrane fusion and the cell cycle: Cdc48p participates in the fusion of ER membranes. *Cell.* 82:885–893.

Lesser, C.F., and C. Guthrie. 1993. Mutational analysis of pre-mRNA splicing in *Saccharomyces cerevisiae* using a sensitive new reporter gene, CUP1. *Genetics.* 133:851–863.

Lippincott, J., and R. Li. 1998. Sequential assembly of myosin II, an IQGAP-like protein, and filamentous actin to a ring structure involved in budding yeast cytokinesis. *J. Cell Biol.* 140:355–366.

Longtine, M.S., and E. Bi. 2003. Regulation of septin organization and function in yeast. *Trends Cell Biol.* 13:403–409.

Longtine, M.S., A. McKenzie III, D.J. Demarini, N.G. Shah, A. Wach, A. Brachat, P. Philippsen, and J.R. Pringle. 1998. Additional modules for versatile and economical PCR-based gene deletion and modification in *Saccharomyces cerevisiae*. *Yeast.* 14:953–961.

Longtine, M.S., C.L. Theesfeld, J.N. McMillan, E. Weaver, J.R. Pringle, and D.J. Lew. 2000. Septin-dependent assembly of a cell cycle-regulatory module in *Saccharomyces cerevisiae*. *Mol. Cell. Biol.* 20:4049–4061.

Ma, Y., and L.M. Hendershot. 2001. The unfolding tale of the unfolded protein response. *Cell.* 107:827–830.

Matlack, K.E., W. Mothes, and T.A. Rapoport. 1998. Protein translocation: tunnel vision. *Cell.* 92:381–390.

McMaster, C.R. 2001. Lipid metabolism and vesicle trafficking: more than just greasing the transport machinery. *Biochem. Cell Biol.* 79:681–692.

Meldolesi, J., and T. Pozzan. 1998. The endoplasmic reticulum Ca^{2+} store: a view from the lumen. *Trends Biochem. Sci.* 23:10–14.

Mino, A., K. Tanaka, T. Kamei, M. Umikawa, T. Fujiwara, and Y. Takai. 1998. Shs1p: a novel member of septin that interacts with spa2p, involved in polarized growth in *Saccharomyces cerevisiae*. *Biochem. Biophys. Res. Commun.* 251:732–736.

Newman, A.P., J. Shim, and S. Ferro-Novick. 1990. BET1, BOS1, and SEC22 are members of a group of interacting yeast genes required for transport from the endoplasmic reticulum to the Golgi complex. *Mol. Cell. Biol.* 10:3405–3414.

Nikonov, A.V., E. Snapp, J. Lippincott-Schwartz, and G. Kreibich. 2002. Active translocon complexes labeled with GFP–Dad1 diffuse slowly as large polysome arrays in the endoplasmic reticulum. *J. Cell Biol.* 158:497–506.

Pelham, H.R. 1991. Recycling of proteins between the endoplasmic reticulum and Golgi complex. *Curr. Opin. Cell Biol.* 3:585–591.

Preuss, D., J. Mulholland, C.A. Kaiser, P. Orlean, C. Albright, M.D. Rose, P.W. Robbins, and D. Botstein. 1991. Structure of the yeast endoplasmic reticulum: localization of ER proteins using immunofluorescence and immunoelectron microscopy. *Yeast.* 7:891–911.

Prinz, W.A., L. Grzyb, M. Veenhuis, J.A. Kahana, P.A. Silver, and T.A. Rapoport. 2000. Mutants affecting the structure of the cortical endoplasmic reticulum in *Saccharomyces cerevisiae*. *J. Cell Biol.* 150:461–474.

Pruyne, D., and A. Bretscher. 2000a. Polarization of cell growth in yeast. *J. Cell Sci.* 113:571–585.

Pruyne, D., and A. Bretscher. 2000b. Polarization of cell growth in yeast. I. Establishment and maintenance of polarity states. *J. Cell Sci.* 113:365–375.

Qureshi, N., R.E. Dugan, W.W. Cleland, and J.W. Porter. 1976. Kinetic analysis of the individual reductive steps catalyzed by beta-hydroxy-beta-methylglutaryl-coenzyme A reductase obtained from yeast. *Biochemistry.* 15:4191–4207.

Sandmann, T., J.M. Herrmann, J. Dengjel, H. Schwarz, and A. Spang. 2003. Suppression of coatomer mutants by a new protein family with COPI and COPII binding motifs in *Saccharomyces cerevisiae*. *Mol. Biol. Cell.* 14:3097–3113.

Segal, M., K. Bloom, and S.I. Reed. 2000. Bud6 directs sequential microtubule interactions with the bud tip and bud neck during spindle morphogenesis in *Saccharomyces cerevisiae*. *Mol. Biol. Cell.* 11:3689–3702.

Shepard, K.A., A.P. Gerber, A. Jambhekar, P.A. Takizawa, P.O. Brown, D. Herschlag, J.L. DeRisi, and R.D. Vale. 2003. Widespread cytoplasmic mRNA

transport in yeast: identification of 22 bud-localized transcripts using DNA microarray analysis. *Proc. Natl. Acad. Sci. USA.* 100:11429–11434.

Sheu, Y.J., Y. Barral, and M. Snyder. 2000. Polarized growth controls cell shape and bipolar bud site selection in *Saccharomyces cerevisiae*. *Mol. Cell. Biol.* 20:5235–5247.

Shulewitz, M.J., C.J. Inouye, and J. Thorner. 1999. Hsl7 localizes to a septin ring and serves as an adapter in a regulatory pathway that relieves tyrosine phosphorylation of Cdc28 protein kinase in *Saccharomyces cerevisiae*. *Mol. Cell. Biol.* 19:7123–7137.

Spang, A., and R. Schekman. 1998. Reconstitution of retrograde transport from the Golgi to the ER in vitro. *J. Cell Biol.* 143:589–599.

Takizawa, P.A., J.L. DeRisi, J.E. Wilhelm, and R.D. Vale. 2000. Plasma membrane compartmentalization in yeast by messenger RNA transport and a septin diffusion barrier. *Science.* 290:341–344.

Waddle, J.A., T.S. Karpova, R.H. Waterston, and J.A. Cooper. 1996. Movement of cortical actin patches in yeast. *J. Cell Biol.* 132:861–870.